Preparation and Characterization of Poly(vinyl chloride)/ Layered Double Hydroxides Nanocomposite via *In Situ* Suspension Polymerization

Yong-Zhong Bao, Zhi-Ming Huang, Zhi-Xue Weng

State Key Laboratory of Polymer Reaction Engineering, Zhejiang University, Hangzhou, 310027 China

Received 28 November 2005; accepted 12 February 2006
DOI 10.1002/app.24317
Published online in Wiley InterScience (www.interscience.wiley.com).

ABSTRACT: Poly(vinyl chloride)/layered double hydroxides (PVC/LDHs) composite resins were prepared by *in situ* suspension polymerization of vinyl chloride monomer in the presence of LDHs intercalated with dodecyl sulfate anions (LDH-DS), and were further processed to obtain PVC/LDH-DS nanocomposites. It was found that the mean particle size of PVC composite resins decreased as LDH-DS was added in the polymerization system. The 5 and 10% weight loss temperatures of PVC resins significantly increased with the increase of LDH-DS weight fraction in the composite resins. The transmission electron microscopy images showed that LDH-DS particles were partially intercalated and partially exfoliated, and well distributed in the PVC nanocomposites. The storage modulus below the glass transition region and the glass temperature of the PVC/LDH-DS nanocomposites are greater than that of the pristine PVC. The mechanical properties of PVC/LDH-DS nanocomposites indicate that LDH-DS nanoparticles stiffen and toughen PVC. The tensile strength, Young's modulus, and Charpy notched impact strength of the PVC/LDH-DS nanocomposites are greater than those of the pristine PVC and PVC/LDH-DS composites prepared by the melt blending. © 2006 Wiley Periodicals, Inc. J Appl Polym Sci 102: 1471–1477, 2006

Key words: poly(vinyl chloride); nanocomposite; layered double hydroxides; morphology

INTRODUCTION

Poly(vinyl chloride) (PVC) is an extensively used thermoplastic material because of its flame retardance, high chemical resistance, and good performance in respect of mechanical behavior as well as low price.[1,2] The successful application of clay, especially montmorillonite (MMT), in the preparation of polymer nanocomposite with excellent properties opens a novel approach to improve the performance of PVC. Wang et al.[3,4] prepared PVC/clay nanocomposites by melt blending of the polymer with an organically modified clay, both in the presence and absence of di(2-ethylhexyl) phthalate (DOP) plasticizer, and found that the tensile strength of the nanocomposite increased as the fraction of clay increased. Yalcin and Cakmak[5] also prepared PVC/clay nanocomposite by melt blending, and found that DOP plasticizer would help the exfoliation and dispersion of clay particles when DOP fraction was suitable. Wan et al.[6,7] found that the partially intercalated and partially exfoliated MMT/PVC nanocomposite could be obtained by melt blending of PVC with alkyl quaternary ammonium modified MMT. The nanocomposites showed better mechanical properties than pristine PVC. However, the nanocomposites were easy to discolor during processing due to the decomposition of alkyl quaternary ammonium. Gong et al.[8,9] reported the synthesis and thermal properties of PVC/MMT nanocomposites via *in situ* intercalative polymerization process. They also confirmed that the presence of the quaternary ammonium in the nanocomposites was responsible for the accelerated degradation of PVC in the initial stage. Accordingly, in this study, a synthetic clay, the so-called layered double hydroxides (LDHs), which has thermal stabilization effect on PVC, is used as an inorganic material in preparing the PVC/clay nanocomposites.

LDHs or hydrotalcite-like materials are a class of anionic clays whose general formula is $[M(II)_{1-x}M(III)_x(OH)_2]^{x+}[A^{n-}_{x/n}\cdot mH_2O]^{x-}$, where M(II) and M(III) represent divalent and trivalent cations, respectively. The interlayer anion (A^{n-}) may be varied over a wide range and the value of the stoichiometric coefficient (x) should be between 0.2 and 0.33.[10] LDHs can absorb and react with HCl produced during the thermal degradation of PVC, thus improve the thermal stability of PVC.[11] Lin et al.[12] found that Mg-Al-CO_3 LDH with Mg/Al = 2 (molar ratio) had the best stabilizing effect on PVC because of its higher layer charge density and

Correspondence to: Y.-Z. Bao (yongzhongbao@zju.edu.cn).
Contract grant sponsors: Zhejiang Science and Technology Department and Quzhou Science and Technology Burean; Contract grant sponsor: Juhua group Corporation; Contract grant number: 2005C11039.

consequently stronger driving force for uptake of Cl^- in the interlayer galleries. Wang and Zhang[13] used micron-sized Mg-Al-CO_3 LDH particles to modify PVC via melt blending, and investigated the effect of LDH on the thermal stability, mechanical properties, rheology, and flame retardance of PVC. Although the thermal stability and flame retardance of PVC were improved as the coupling agent treated LDH incorporated, the tensile and impact strength of PVC composite decreased as the weight fraction of incorporated LDH increased.

Although the intercalated LDHs/polymer nanocomposites associated with water-soluble polymers have been successfully prepared in several investigation using coprecipitation,[14] ion exchange,[15,16] and *in situ* polymerization methods,[17,18] only few reports are available on the intercalated or exfoliated LDHs/water-insoluble polymer nanocomposites, since the layers of LDHs are tightly stacked by the strong attractive force among the interlayer anions. This situation does not favor exfoliation. Recently, Qu et al. successfully synthesized exfoliated LDHs/PE-*g*-MA[19] and LDHs/LLDPE[20] nanocomposites by refluxing in a nonpolar xylene solution of PE-*g*-MA and LLDPE, respectively. Chen et al. prepared the exfoliated LDHs/polyimide,[21] LDHs/epoxy,[22] and LDHs/PMMA[23] nanocomposites by *in situ* polymerization. However, PVC/LDHs nanocomposite has never before been investigated.

In this work, LDHs intercalated with dodecyl sulfate (DS) anion was prepared by coprecipitation method, and PVC/LDHs nanocomposites were prepared by vinyl chloride monomer (VCM) suspension polymerization in the presence of the modified LDHs, and by the followed melt processing of the composite PVC resin. The morphology, thermal, and mechanical properties of the resulting nanocomposites will be investigated and compared with PVC/LDHs composite prepared by the direct melt blending.

EXPERIMENTAL

Materials

The materials used in the synthesis of the dodecyl sulfate (DS) intercalated LDHs were $Mg(NO_3)_2{\cdot}6H_2O$ (Shanghai Chemical Reagents, China), $Al(NO_3)_3{\cdot}9H_2O$ (Shanghai Chemical Reagents,), NaOH (Hangzhou Chemical Reagents, China), and sodium dodecyl sulfate (Shanghai Chemical Reagents) both in analytical reagent grade and used without further purification. LDHs with the formula of $Mg_{0.67}Al_{0.33}(OH)_2(CO_3)_{0.17}{\cdot}2H_2O$ (LDH-CO_3) was supplied by Fumeida New Materials, Dalian, China.

Vinyl chloride monomer (VCM) was of polymerization grade, and supplied by Hangzhou Electro-chemical, China. Partially hydrolyzed poly(vinyl alcohol) (PVA, KH20) and hydroxylpropylmethyl cellulose (HPMC, 65SH50) were purchased from the Synthesis Chemical Company of Japan (Osaka, Japan). The diethylhexyl peroxydicarbonate (EHP) (in the form of solution with concentration of 75%) initiator was provided by Akzo Chemical, Tianjin, China. Organtin (ZT-203) and epoxy soybean oil (ESO) thermal stabilizers were of commercial grade.

Preparation of Mg/Al LDHs intercalated with DS anion

The Mg/Al LDHs intercalated with DS anion were synthesized by the coprecipitation method. The preparation was carried out in an N_2 atmosphere to exclude carbonate from the LDHs. Magnesium nitrate (0.2 mol) and aluminum nitrate (0.1 mol) were dissolved in 500 mL of double deionized water. The nitrate solution was then slowly dropped into vigorously stirred 500 mL water solution of sodium dodecyl sulfate (0.2 mol). The pH value of the solution was maintained at 10 by adding 1*M* NaOH solution. After the addition of nitrate solution, the resulting precipitate was aged at 80°C for 12 h, and was filtered until all the supernatant liquid was removed. The sample was washed several times by double deionized water and dried at 50°C in a vacuum oven for 24 h.

Preparation of PVC/LDH-DS composites

Preparation of PVC/LDH-DS nanocomposite by in situ suspension polymerization

The PVC/LDH-DS nanocomposites were prepared through *in situ* suspension polymerization and subsequent melt processing. The polymerizations were carried out in a 5 L stainless steel autoclave, fitted with an agitator consisting of a two-flat-blade impeller and a two-45° inclined-blade impeller. The "reverse-feeding" mode was adopted in the preparation of PVC/LDH-DS composite resin, that is, accurately weighed amount of LDH-DS, 1.0 g EHP, and 1000 g of VCM were placed in the autoclave first. The mixture was then stirred vigorously at room temperature for 1 h to achieve good dispersion of LDH-DS in the VCM. After this, 2000 g of distilled water, suspending agents PVA (0.7 g) and HPMC (0.7 g) were introduced into the reactor by using a metering pump and stirred for 1 h. Then, the system was heated to 57°C to start the polymerization. The pressure of the polymerization system was maintained at about 9.7 kg/cm^2 before the pressure drop and the polymerization was terminated when 2.0 kg/cm^2 pressure drop was achieved. After venting the residual monomer, the resin was recovered by filtration and dried at 60°C for about 24 h. The polymerization conversion of VCM was determined by weighing method, and the weight fraction of LDH-DS in the composite resin was calculated from the

initial weight of LDH-DS added and the weight of the obtained composite resin.

The mixture of 100 g PVC/LDH composite resin, 3.5 g organotin, and 1.5 g ESO was milled in a HAAKE 90 Torque Rheometery for 5 min. The initial temperature was set at 180°C and the rotor speed at 50 rpm. The processed mixtures were then molded into 4 mm sheets in a laboratory press at 185°C and 30 MPa for 10 min, followed by cooling to room temperature at pressure to obtain samples for characterization.

Preparation of PVC/LDH-DS composite by direct melt blending

The mixture of 100 g pure PVC, LDH-DS (at the same level as for *in situ* polymerization resin), 3.5 g organotin, and 1.5 g ESO was milled in the HAAKE Rheometery for 5 min, and molded into 4 mm sheets, under the same processing conditions as described earlier.

Characterization

The X-ray diffraction (XRD) patterns were determined using a XRD-6000 X-ray diffractometer (Shimadzu, Japan), using Cu Kα radiation (λ = 0.1542 nm), at a scanning rate of 4° min^{-1} over 2θ intervals from 3 to 70°. The FTIR spectra were recorded on a Perkin-Elmer System 2000 Fourier transform infrared spectrophotometer with a spectral resolution of 4 cm^{-1}. Transmission electron microscopy (TEM) images were taken from cryogenically microtomed ultrathin sections using a JEM-1230 transmission electron microscope (JEOL, Japan).

The particle size of LDHs and PVC resins was measured by using a Coulter laser particle size analyzer (Coulter LS-230). The molecular weight and molecular weight distribution of PVC was measured by using a Waters 150C GPC, equipped with three polystyrene gel columns (10^3, 10^4, 10^5 nm), at a flow rate of 1 mL/min in tetrahydrofuran at 25°C. Polystyrene standard samples with narrow molecular weight distribution were used as standards. Thermogravimetric analysis (TGA) was performed to determine the thermal degradation of PVC and PVC/LDH-DS composite resins using a Perkin-Elmer Pyris-1 TGA analyzer at a heating rate of 10°C/min under N_2 atmosphere.

Dynamic mechanical analysis (DMA) was performed using a Du-Pont 2980 Instrument dynamic mechanical analyzer at a fixed frequency of 10 Hz in a temperature range from 30 to 120°C, and the heating rate was 2°C/min. Charpy notched impact strength was measured by using a CEAST impact tester according to China National Standard GB1043–93. The tensile properties were determined by using a Zwick/Roell Z202 universal testing machine according to Chinese National Standard GB1040–92. All the tests were done at (23 ± 2)°C, and more than five measurements were carried out for each data point.

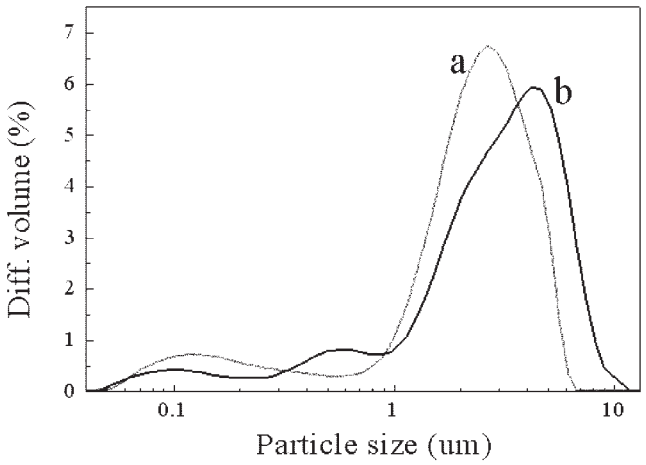

Figure 1 Particle size distribution of (a) LDH-CO_3 and (b) LDH-DS.

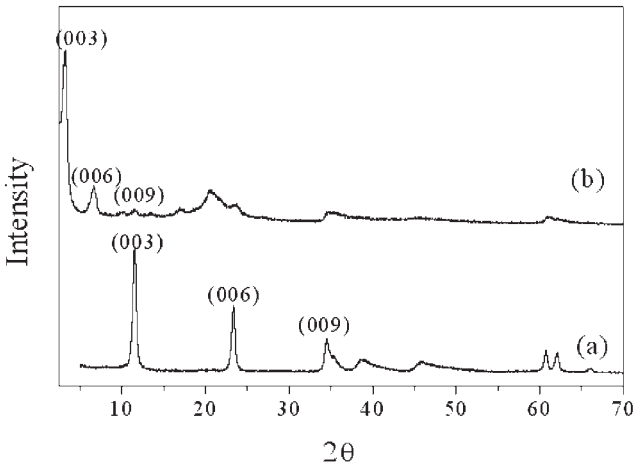

Figure 2 XRD diffraction patterns of (a) LDH-CO_3 and (b) LDH-DS.

RESULTS AND DISCUSSION

Characterization of LDH-DS

The intercalation of DS into LDH could improve the compatibility of LDH with VCM and expend the layer spacing, which would be a further benefit for the incorporation of LDH particles into VCM droplets in suspension polymerization, and intercalation or exfoliation of LDH by PVC chains.

Figure 1 presents the size distributions of the LDH-CO_3 and the LDH-DS in aqueous phase. It can be seen that the size of most LDHs particles range from 1 to 10 μm.

Figure 2 presents the XRD patterns of the LDH-CO_3 and the LDH-DS. The XRD pattern of the LDH-DS demonstrates that the diffraction peak of 003 shown in

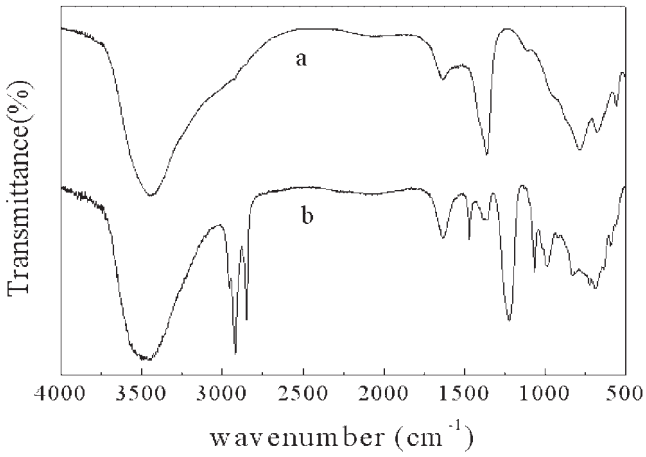

Figure 3 FTIR spectra of (a) LDH-CO_3 and (b) LDH-DS.

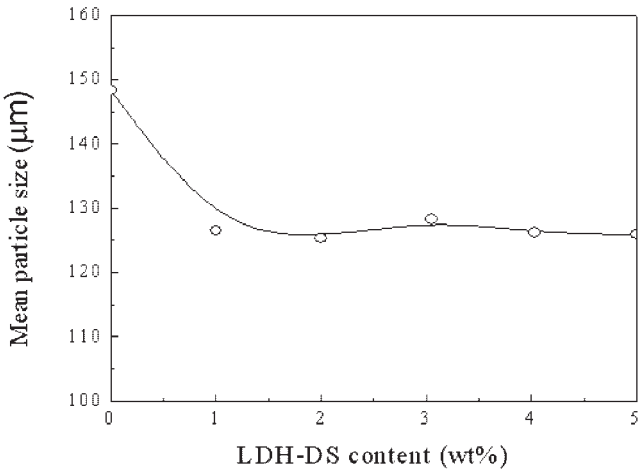

Figure 4 Effect of LDH-DS on the mean particle size of resins.

pattern of the LDH-CO_3 is disappeared, and the strongest diffraction peak appears at $2\theta = 3.24°$. The result reveals that the maximum basal spacing of LDH-DS is 27.3 Å, while that of LDH-CO_3 is 7.8 Å. The increase of basal spacing of the LDH-DS demonstrated that the DS anion, which has a large volume, was effectively intercalated into the interlayer of LDH. Additionally, the existence of diffraction peaks of 006 and 009 indicates that the layer characteristic of the LDH-DS is extremely pronounced.

Figure 3 shows the FTIR spectra of the LDH-DS and LDH-CO_3. A strong peak at 1365 cm^{-1} appeared in Curve *a* is associated with the asymmetric stretching vibration of the carbonate anions.[24] The fingerprint peaks at 610 and 430 cm^{-1} are associated with O—M—O stretching modes in the LDHs sheets.[25] The FTIR spectrum of the LDH-DS contains strong absorption at 1197 and 1049 cm^{-1} are assigned to the stretching vibrations of RSO_4^-. The characteristic peaks associated with vibration of —CH_3 and —CH_2 groups occur at 2850–2950 cm^{-1}. These FTIR assignments further confirm that DS anion is successfully intercalated into the gallery of the LDH.

Characterization of PVC/LDH-DS composite resin prepared by *in situ* suspension polymerization

Pure PVC and PVC/LDH-DS composite resins were synthesized under the same polymerization condition and the conversion of VCM to PVC was controlled to be (80 ± 2)%. The effect of LDH-DS on the mean particle size of PVC resins is shown in Figure 4. It can be seen that the mean particle sizes of PVC composite resins are all smaller than that of pure PVC resin, and the particle size has no obvious change as the weight fraction of LDH-DS increased.

After the separation of LDH-DS by micro-filtrating of PVC solution, the molecular weight (MW) and molecular weight distribution (MWD) of PVC resins were measured. The influence of LDH-DS weight fraction on the number average MW (M_n), weight average MW (M_w), and the index of MWD (M_w/M_n) are shown in Table I. It shows that M_w and MWD of PVC change no more as the weight fraction of LDH-DS increased.

From TGA curves of pristine PVC and PVC/LDH-DS composite resins, the 5 and 10% weight loss temperatures ($T_{5\%}$ and $T_{10\%}$) were obtained. The influence of LDH-DS weight fraction on $T_{5\%}$ and $T_{10\%}$ is shown in Figure 5.

It can be seen that $T_{5\%}$ and $T_{10\%}$ increase with the increase of LDH-DS content in the composite resin. Thermal dehydrochlorination is the main weight loss in the initial thermal degradation stage of PVC, and the produced HCl has an acceleration action on the further decomposition of PVC.[26] LDH-DS in the composite resin can absorb and react with produced HCl. As a result, the degradation rate of PVC decreased and the temperature corresponding to a certain weigh loss increased.

Morphology of PVC/LDH-DS composites

Figure 6 shows TEM micrographs of PVC/LDH-DS composites prepared by the melt blending, and by *in*

TABLE I
Effect of LDH-DS on the Molecular Weight and Molecular Weight Distribution of PVC

Sample	M_n	M_w	M_w/M_n
Pure PVC	46,742	90,608	1.94
PVC/LDH-DS (1 wt %)	45,351	91,155	2.01
PVC/LDH-DS (2 wt %)	46,131	90,878	1.97
PVC/LDH-DS (3 wt %)	44,284	90,340	2.04
PVC/LDH-DS (4 wt %)	44,118	90,884	2.06

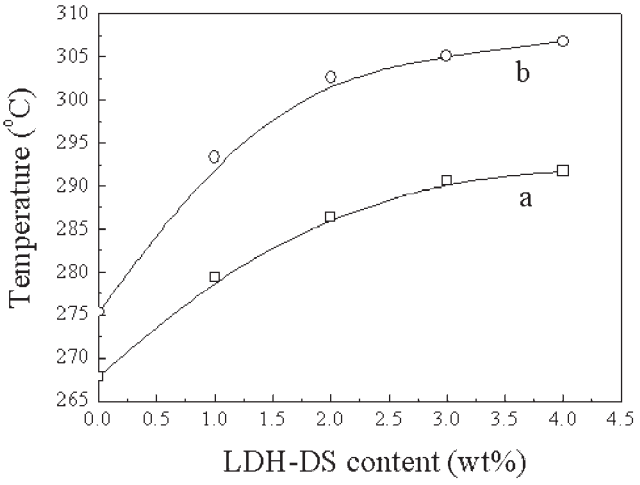

Figure 5 Effect of LDH-DS content on the (a) 5% and (b) 10% weight loss temperatures of PVC.

situ suspension polymerization and subsequent melt processing.

It can be seen that the size of dispersed LDH-DS particles is greater (>100 nm), and the particles are hardly intercalated or exfoliated in PVC/LDH-DS composite prepared by the direct melt blending. This illustrate that the attraction force of LDH-DS layers is still strong and it is difficult for PVC chains to intercalate in the melt blending process. In Figures 6(b) and 6(c), the dark strips correspond to LDHs layers. The TEM images show that the LDHs layers are well dispersed in the PVC matrix and much strongly oriented. The size of dispersed LDHs particles is smaller than the size of the original LDHs particles as shown in Figure 1. Particularly, the thickness of LDHs layers ranges from 10 to 50 nm, which is much smaller than the length of LDHs particles, but is still greater than the thickness of the individual LDHs layer. So, only the partially intercalated and partially exfoliated LDH-DS/PVC nanocomposites were prepared by *in situ* suspension polymerization and subsequently melt processing. This is similar to the situation of PVC/MMT nanocomposites reported by Wan et al.[6]

Dynamic mechanical properties of PVC/LDH-DS nanocomposites

Figure 7 shows the variation of storage modulus (E') with temperature for pristine PVC and PVC/LDH-DS nanocomposites containing 1 and 3 wt % LDH-DS. It

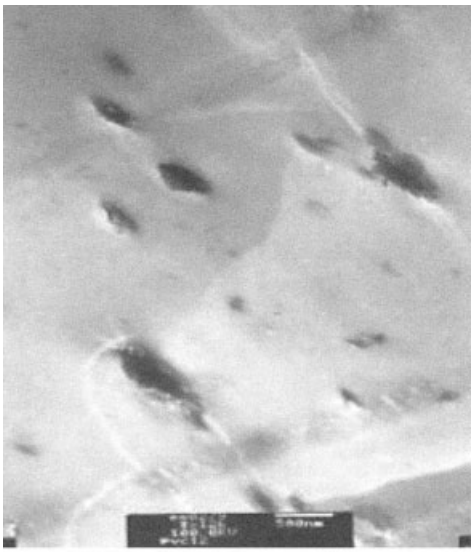

(a)

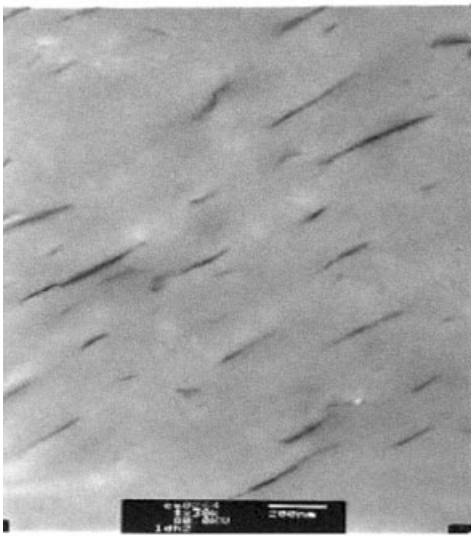

(b)

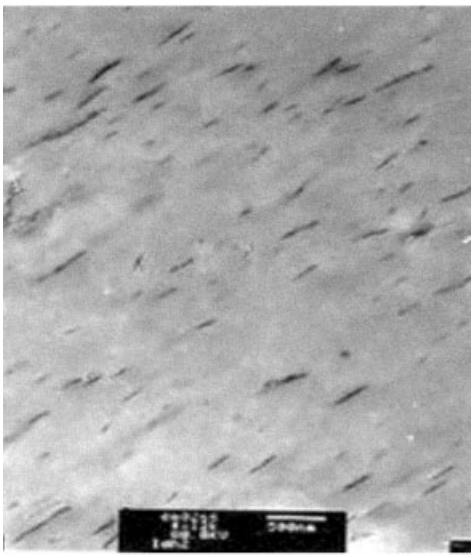

(c)

Figure 6 TEM micrographs of PVC/LDH-DS composites prepared by the direct melt blending (a: LDH-DS 3%, scale bar 500 nm), and *in situ* suspension polymerization and melt processing (b: LDH-DS 1%, scale bar 200 nm, c: LDH 3%, scale bar 500 nm).

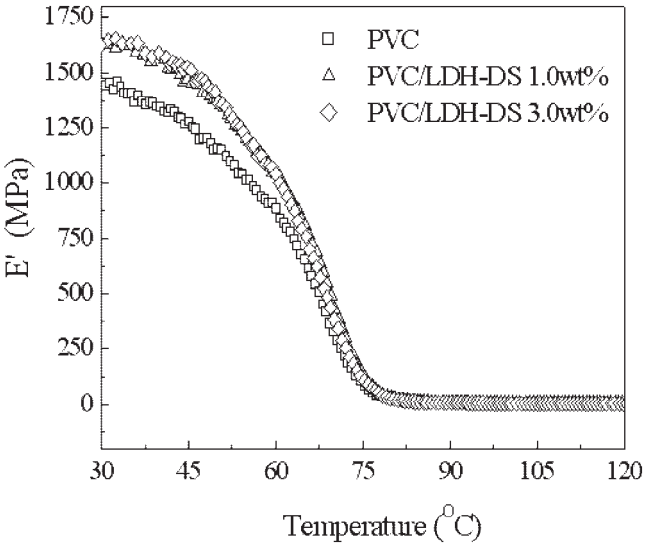

Figure 7 Variation of E' with temperature for PVC and PVC/LDH-DS nanocomposites.

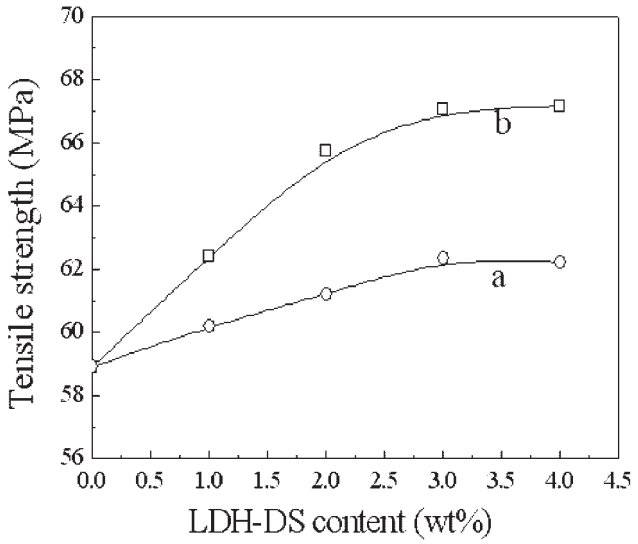

Figure 9 Influence of LDH-DS weight fraction on tensile strength of PVC/LDH-DS composites: (a) melt blending; (b) *in situ* polymerization.

can be seen that the E' of PVC/LDH-DS nanocomposites are all greater than that of pristine PVC below the glass transition region. In addition, the E' of the two PVC/LDH-DS nanocomposites is similar to each other. While the three samples show no obvious difference in the E' in the rubber plateau region. These phenomena are similar to that of PVC/MMT[6] and PVC/$CaCO_3$ nanocomposites.[27]

Figure 8 shows the variation of tan δ with temperature for PVC and PVC/LDH-DS nanocomposites. The glass transition temperatures (T_g) of the PVC phases in pristine PVC and PVC/LDH-DS nanocomposites with 1 and 3 wt % are 79.9, 80.9, and 81.6°C, which confirms that well dispersed nanosheets restrict the motion of PVC segmental chains.

Mechanical properties of PVC/LDH-DS composites

Influences of LDH-DS weight fraction on the tensile strength and Young's modulus of the melt blending PVC/LDH-DS composites and PVC/LDH-DS nanocomposites prepared by *in situ* polymerization are shown in Figures 9 and 10, respectively.

It can be seen that both the tensile strength and Young's modulus increase with the increase of LDH-

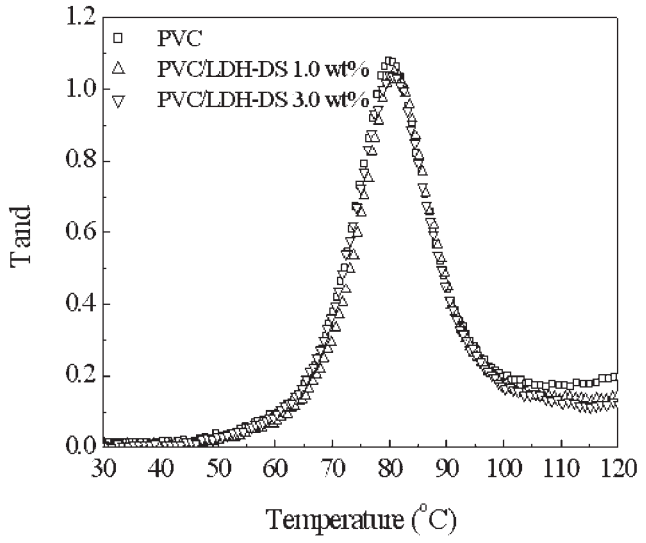

Figure 8 Variation of tan δ with temperature for PVC and PVC/LDH-DS nanocomposites.

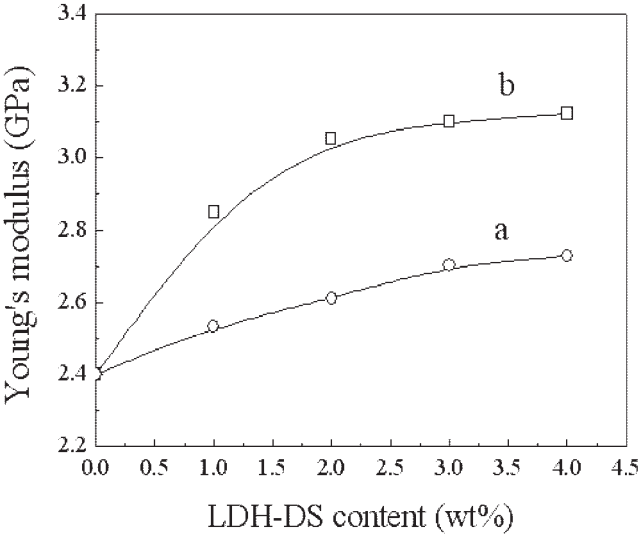

Figure 10 Influence of LDH-DS weight fraction on Young's modulus of PVC/LDH-DS composites: (a) melt blending; (b) *in situ* polymerization.

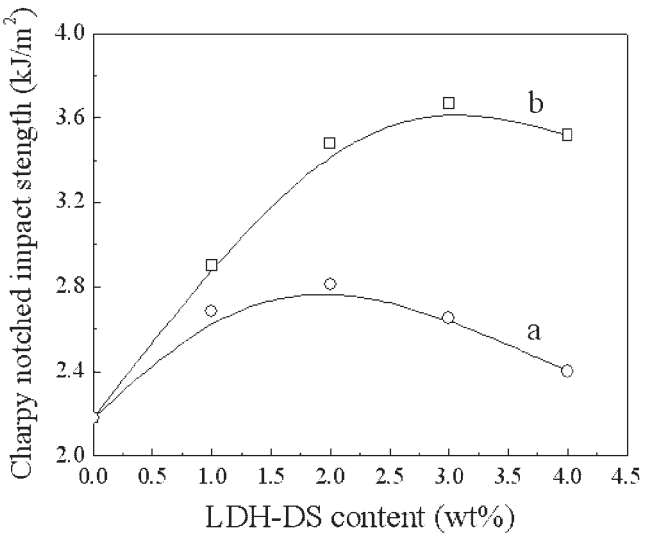

Figure 11 Variation of Charpy notched impact strength of PVC/LDH-DS composites with the weight fraction of LDH-DS: (a) melt blending PVC/LDH-DS composite; (b) *in situ* polymerization.

DS weight fraction for the melt blending PVC/LDH-DS composites and PVC/LDH-DS nanocomposites prepared by *in situ* polymerization, but the tensile strength and Young's modulus of PVC/LDH-DS nanocomposites are greater than those of the melt blending PVC/LDH-DS composites at the same weight fraction of LDH-DS. This was caused by the better stiff enhancement of the partially intercalated and partially exfoliated LDH-DS on PVC.

Figure 11 shows the variation of Charpy notched impact strength with the weight fraction of LDH-DS for the melt blending PVC/LDH-DS composites and PVC/LDH-DS nanocomposites prepared by *in situ* polymerization. Obviously, the impact strength of all nanocomposites is greater than that of pure PVC and of the melt blending PVC/LDH-DS composites. As the LDH-DS weight fraction is increased to 3.0 wt %, the Charpy impact strength reaches a maximum. Further increase in LDH-DS loading gives lower impact strength.

CONCLUSIONS

DS can be intercalated into the interlayers of LDH layers by the coprecipitation method. PVC/LDH-DS composite resins were successfully synthesized by *in situ* suspension polymerization of VCM in the presence of LDH-DS, and further processed to obtain PVC/LDH nanocomposites. The addition of LDH-DS led the decrease of the mean particle size of PVC composite resins, and had no obvious influence on the molecular weight and molecular weight distribution of PVC. The 5 and 10% weight loss temperatures of PVC significantly increased with the increase of LDH-DS weight fraction in the composite resins. LDH-DS particles were partially intercalated and partially exfoliated, and well distributed in the PVC nanocomposite, while LDH-DS is hardly intercalated and exfoliated by melt blending of PVC with the LDH-DS. The DMA results indicate that the storage modulus below the glass transition region and the T_g of the PVC/LDH-DS nanocomposites are greater than that of the pristine PVC. It indicates that LDH nanoparticles stiffen and toughen PVC. The tensile strength, Young's modulus, and Charpy notched impact strength of the PVC/LDH-DS nanocomposites are greater than those of the pristine PVC and the melt blending PVC/LDH-DS composites. The optimal mechanical properties were obtained at 3 wt % loading of LDH-DS nanoparticles in the PVC/LDH-DS nanocomposite.

References

1. Allsoapp, M. W. In Manufacture and Processing of PVC; Burgess, R. H., Ed.; Applied Science: London, 1982; p 152.
2. Smallwood, P. V. In Encyclopedia of Polymer Science and Engineering, 2nd ed.; Mark, H. F., Bikales, N. M., Overberger, C. G., Eds.; Wiley: New York, 1989; Vol. 17.
3. Wang, D. Y.; Parlow, D.; Yao, Q.; Wilkie, C. A. J Vinyl Add Technol 2001, 7, 203.
4. Wang, D. Y.; Parlow, D.; Yao, Q.; Wilkie, C. A. J Vinyl Add Technol 2002, 8, 139.
5. Yalcin, B.; Cakmak, M. Polymer 2004, 45, 6623.
6. Wan, C. Y.; Qiao, X. Y.; Zhang, Y.; Zhang, Y. X. Polym Test 2003, 22, 453.
7. Wan, C. Y.; Zhang, Y.; Zhang, Y. X. Polym Test 2004, 23, 299.
8. Gong, F. L.; Zhao, C. G.; Feng, M.; Qin, H. L.; Yang, M. S. J Mater Sci 2004, 39, 293.
9. Gong, F. L.; Feng, M.; Zhao, C. G.; Zhang, S. M.; Yang, M. S. Polym Degrad Stab 2004, 84, 289.
10. Cavani, F.; Trifiro, F.; Vaccari, A. Catal Today 1991, 11, 173.
11. van der Ven, L.; van Gemert, M. L. M.; Batenburg, L. F.; Keern, J. J.; Gielgens, L. H.; Koster, T. P. M.; Fischer, H. R. Appl Clay Sci 2000, 17, 25.
12. Lin, Y. J.; Li, D. Q.; Evens, D. G.; Duan, X. Polym Degrad Stab 2005, 88, 286.
13. Wang, X. D.; Zhang, Q. Polym Int 2004, 53, 698.
14. Wilson, O. C., Jr.; Olorunyolemi, T.; Jaworski, A.; Borum, L.; Young, D., et al. Appl Clay Sci 1999, 15, 265.
15. Leroux, F.; Aranda, P.; Besse, J.; Ruiz-Hitzky, E. Eur J Inorg Chem 2003, 6, 1242.
16. Yang, Q. Z.; Sun, D. J.; Zhang, C. C.; Wang, X. J.; Zhao, W. A. Langmuir 2003, 19, 5570.
17. Vieille, L.; Taviot-Gueho, C.; Besse, J. P.; Leroux, F. Chem Mater 2003, 15, 4369.
18. Roland-Swanson, C., Besse, J. P., Leroux, F. Chem Mater 2003, 16, 5512.
19. Chen, W.; Qu, B. Chem Mater 2003, 15, 3208.
20. Chen, W.; Feng, L.; Qu, B. Chem Mater 2004, 16, 368.
21. Hsueh, H. B.; Chen, C. Y. Polymer 2003, 44, 1151.
22. Hsueh, H. B.; Chen C. Y. Polymer 2003, 44, 5275.
23. Wang, G. A.; Wang, C. C.; Chen, C. Y. Polymer 2005, 46, 5065.
24. Iyi, N.; Matsumoto, T.; Kaneko, Y.; Kitamura, K. Chem Mater 2004, 16, 2926.
25. Oriakhi, C. O.; Farr, I. V.; Lerner, M. M. J Mater Chem 1996, 6, 103.
26. Starnes, W. H., Jr. Prog Polym Sci 2002, 27, 2133.
27. Xie, X. L.; Liu, Q. X.; Li, R. K. Y.; Zhou, X. P.; Zhang, Q. X.; Yu, Z. Z.; Mai, Y. W. Polymer 2004, 45, 6665.